ADVANCES IN GEODESY AND GEOINFORMATION
(formerly GEODESY AND CARTOGRAPHY)
Vol. 71, no. 2, article no. e25, 2022
https://doi.org/10.24425/agg.2022.141299

Original paper

Part of Topical collection:
"Advancements in Applied Geoinformatics"

Applying autoregressive models in analysis of GRACE-Mascon time-series

Ozge Gunes*, Cuneyt Aydin

Yildiz Technical University, Istanbul, Turkey,
e-mail: ozgeg@yildiz.edu.tr; ORCID: http://orcid.org/0000-0001-7576-621X
e-mail: caydin@yildiz.edu.tr; ORCID: http://orcid.org/0000-0003-0888-0316

*Corresponding author: Ozge Gunes, e-mail: ozgeg@yildiz.edu.tr

Received: 2022-02-28 / Accepted: 2022-05-09

Abstract: This study discusses how to model the noise in a Gravity Recovery and Climate Experiment (GRACE)-Mascon derived Equivalent Water Thicknesses (EWT) time-series. GRACE has provided unique information for monitoring variations in EWT of continents in regional or basin scale since 2002. To analyze a GRACE EWT time-series, a standard harmonic regression model is used, but usually assuming white noise-only stochastic model. However, like almost all kinds of geodetic time-series, it has been shown that the GRACE EWT time-series contains temporal correlations causing colored noise in the data. As well known in geodetic modelling studies, neglecting these correlations leads to underestimating the uncertainties, and so misinterpreting the significancy of the parameter estimates such as trend rate, amplitudes of signals etc. In this study, autoregressive noise modeling, which has some advantageous compared to the approaches and methods frequently applied in geodetic studies, is considered for GRACE EWT time series. For this aim, three important basins, namely the Yangtze, Murray–Darling and Amazon basins have been examined. Among some applied autoregressive models, the ARMA(1,1) model is obtained as the best-fitting noise model for analyzing the EWT changes in each basin. The obtained results are discussed in terms of forecasting, significancy and consistency with GRACE-FO mission.

Keywords: GRACE Mascon, equivalent water thickness, temporal correlation, colored noise, autoregressive models

1. Introduction

There are two satellite systems that have been used to determine the Earth's gravitation by gradiometric missions: GRACE and GRACE-FO (GRACE Follow-On). Many hydro-geodetic researches that integrate many disciplines, such as monitoring water storage variations in basins, glacier melting, sea level changes and drought, have been carried out thanks to this satellite system, which enables high-precision monitoring of water mass variations (Tapley et al., 2004; Wahr et al., 2006; Cazenave and Chen, 2010; Baur, 2012; Forsberg et al., 2017; Ran et al., 2018; Wang et al., 2020; Chen et al., 2022; Scanlon et al., 2022).

The GRACE product, which is widely used to analyze the change in equivalent water thickness. When modeling the trend derived from this monthly released data set, it is necessary to define appropriate functional and stochastic models. The fact that the structure proposed in stochastic modeling is not designed in accordance with the time-series characteristics may result in misinterpretations over the trend of increasing or decreasing water mass change.

There have been numerous GRACE-related studies to monitor changes in the water mass. These studies have focused on the basins that have an important contribution to the Earth's water cycle (Famiglietti and Rodell, 2013; Birylo et al., 2018; Frappart and Ramillien, 2018; Ahmed et al., 2019; Rahaman et al., 2019; Chao et al., 2021; Huang et al., 2021; Boergens et al., 2022). The Yangtze, Murray–Darling and Amazon basins are only a few examples of these basins. GRACE observations from the studies conducted in these basins were compared to several hydrological models. Using GRACE, it has been possible to monitor the change in the water mass over years, including extreme droughts and floods. Major floods and droughts that occurred in the Yangtze basin have been the subject of many GRACE studies as well as monitoring the equivalent water thickness change. (Yin and Li, 2001; Ferreira et al., 2013; Huang et al., 2015; Zhou et al. 2016; Chao and Wang, 2017; Gao et al., 2017; Sun et al., 2017; Zhang et al., 2019; Chao et al., 2021). Moreover, changes in total water storage in the Amazon and Murray–Darling basins, which are prone to extreme phenomena such as El Nino and La Nina, are examined (Chen at al., 2010; Becker et al., 2011; Frappart et al., 2012; Xie et al., 2016; Heimhuber et al., 2019; Pellet et al., 2021). In these basins, the GRACE observations are compared with a variety of datasets, such as hydro-meteorological factors, climate variables, hydrologic models, and different components of the water cycle (Crowley et al., 2008; Brown and Tregoning, 2010; Fasullo et al., 2013; Schumacher et al., 2018; Frappart et al., 2019; Chen et al., 2020). These studies generally focus on functional modeling of the data set and compatibility of the trend in water mass change with other hydro-climatic factors. When analyzing a time-series, not only the functional part but also the stochastic part is to be modeled realistically (Davis et al., 2012). It is well known that almost all kinds of geodetic time-series contain temporal correlations resulting in colored noise in the data. These correlations should be considered while analyzing time-series to get more realistic estimates, especially for the uncertainty of the trend rate or other parameters studied. The GRACE time-series also contains such temporal correlations as shown in some studies, including Williams et al. (2014), Guo et al. (2018), Loomis et al.

(2019) and King and Watson (2020). In order to evaluate these correlations and model the colored noise in GRACE time-series, maximum likelihood and variance component estimation methods, which are mostly used in geodetic GPS studies, can be applied after prescribing the "noise model" as "white noise+flicker noise", "white noise+flicker noise+random walk noise", etc. These methods, however, may fail in estimating the amplitude of each noise in the assumed model for a GRACE time-series mainly due to low observation frequency, insufficient noise ratio and number of periods in the time-series. As an alternative to these geodetic noise modelling methods, autoregressive models such as AR (AutoRegressive), MA (Moving Average), ARMA (AutoRegressive–Moving-Average), ARIMA (AutoRegressive Integrated Moving Average) etc. may provide more flexibility in the noise definition since they need only specifying the relationships between observations at some specific lags in the time-series such that the residuals become stationary as a result of the analysis. This study, therefore, considers the autoregressive noise modeling with ARMA/ARIMA model in GRACE EWT time-series to have realistic estimates for the trend in the EWT changes in selected Yangtze, Murray–Darling and Amazon basins as a numerical example. The paper's research aim is to investigate the most fitting model by examining how the standard errors of the trend vary under different models with respect to the colored noise.

This study is organized as follows: the next section briefly explains the GRACE data used herein, harmonic regression model for the EWT changes, colored noise, and used tools for autoregressive models. In the Results and Discussion section, the obtained results for the basins with ARMA/ARIMA models are discussed. The final section concludes our study.

2. Materials and methods

The GRACE satellite system, which was operated in collaboration with NASA and DLR (Deutsches Zentrum für Luft- und Raumfahrt), provided data from 2002 to 2017. The system, which consists of twin satellites with a distance of 220 ± 50 kilometers between them, is orbiting in an orbit with an altitude of around 500 kilometers and an inclination of 89.5 degrees with respect to the equator (Tapley et al., 2004). The GRACE satellite, its measuring principle is based on the change in distance between the twin satellites (K-Band Ranging, KBR), accomplishes its mission in approximately 30 days. As a result of precise monitoring of KBR changes, it is possible to observe the gravity change and the corresponding water storage change solutions with high precision (a spatial resolution of about 300 km). GRACE-FO was launched into orbit in 2018 as a successor to GRACE. It has a similar design of GRACE with a distance of approximately 220 kilometers between twin satellites and an altitude of approximately 490 kilometers (Tapley et al., 2019).

The solutions obtained from GRACE and GRACE-FO observations are presented to users as products of different levels (Level-1 to Level-4). One of them, Level-3 Mascon solutions is also published as monthly EWT changes for surface gridded of different resolutions by various data centers including Center for Space Research (CSR), GSFC and Jet Propulsion Laboratory (JPL). Mascon is essentially a gravitational field function

derived from GRACE twin satellite observations, each of which represents mass concentrations distributed throughout the earth's surface. GSFC Mascon solutions consist of 41168 equal-area mascon cells with a 1 arc-degree (Luthcke et al., 2013; Loomis et al, 2019). In addition to 1 arc-degree cells, basins and regions are also represented in mascon solutions. These solutions are generated using different background models. For instance, the Glacial Isostatic Adjustment (GIA) correction performed by ICE-6G D (Peltier et al., 2015) and the C_{20} and C_{30} coefficient replacements made by Loomis et al. (2020). As a static background field GGM05C is used (Ries et al., 2016) and atmosphere and ocean de-aliasing effect removed by Dobslaw et al. (2017).

The most recent mascon solutions provided by the GSFC are released in version RL06 v1.0 comprising monthly EWT changes for the period April 2002 to October 2021 (163 months for GRACE period of 2002-2017). Background models, details and all data sets are available at the Goddard Earth Science Research GRACE Mascon Current Products webpages (https://earth.gsfc.nasa.gov/geo/data/grace-mascons). EWT, which is based on monthly gravity field solutions, is a geopotential function that has a trend and a periodic component. The functional model used in modeling EWT change is given by:

$$y(t_j) = a + bt_j + \sum_{i=1}^{m} \left\{ c_i \cos(\omega_i t_j) + s_i \sin(\omega_i t_j) \right\}, \tag{1}$$

where $y(t_j)$ corresponds to the EWT changes, a denotes the shift, b stands for the annual trend, c and s are the cosine and sine amplitudes of the corresponding sinus signal, respectively, m is the number of the periodic signals and ω is the sinusoidal signal's angular frequency. It is defined as $2\pi/T_i$ with respect to the period T. Here, the period T_i corresponds to annual and semiannual signals. This model is known as the harmonic regression approach. The annual change in water storage can be estimated using the least-square adjustment.

When modeling the stochastic component of a time-series, it is necessary to investigate temporal correlations in order to obtain realistic standard errors. If these correlations are neglected, estimated time-series parameters, particularly their standard errors (uncertainties), may be underestimated. For this reason, trying to figure out if there are any temporal correlations and how to properly weight the observations is the most essential part of stochastic modelling. Various methods are used to investigate the temporal correlations. The analysis of the spectral density function (PSD) is one of them. Time-series spectral analysis is described as the examination of the PSD in the frequency domain (Chatfield, 2003; Brockwell and Davis, 2016). It should be emphasized that white noise is not the only noise type in the dataset. A time-series may also include noise types with different spectral indices, like colored noise or power law noise.

The power spectrum of this noise is equal to the power law described by (Welch, 1967; Mandelbrot and Van Ness, 1968):

$$\mathrm{PSD}(f) = P_0 \left(\frac{f}{f_0} \right)^{\kappa}. \tag{2}$$

The spectral index is denoted by κ; the normalization constants are represented by P_0 and f_0. According to the spectral index value, $\kappa = 0$ was defined as white noise (WN);

$\kappa = -1$ as flicker noise (FN); and $\kappa = -2$ as random walk noise (RWN). Besides of integer noise types, those with a range of $-3 < \kappa < -1$ is referred to as fractional Brownian motion, while those with a range of $-1 < \kappa < 1$ is referred to as fractional Gaussian noise. When periodograms are made by plotting decibel values against the natural logarithm of frequency, the slope of the line corresponds to the noise's spectral index, and the noise type can be specified in the spectrum. This is called a "log–log graph".

Autoregressive models are used to handle the colored noise existing in time-series. A linear combination of estimators is used to estimate the variable of interest in the regression model. In an autoregression model, the variable of interest is forecasted using a linear combination of prior values. The term autoregression implies that the variable is being regression against itself. As a result, a p-order autoregressive model can be stated as AR(p). In a regression model, if the prior forecast errors are employed, this model implies a q-order moving average model defined as MA(q). The case in which the value of any period of a time-series is described as a combination of a certain number of prior observation values plus error terms is denoted as an Autoregressive Moving Average ARMA(p, q). Here, p and q symbolize the order of the autoregressive and moving average parts, respectively. Thus, the characteristics of autoregressive and moving average models are integrated into a single model. By combining the autoregression, first order differentiation, and moving average models, an ARIMA (Autoregressive Integrated Moving Average) is formed. In the ARIMA(p, d, q) model, d specifies the first degree of differentiation. All of the parameters p, d, and q are non-negative integers. The autocorrelation function (ACF) and partial autocorrelation function (PACF) plots have been used to determine the p and q orders in the models. The use of an ARMA model can be used when neither the autocorrelations nor the partial autocorrelations are cut off by a few lags.

The information criteria are also important for deciding which ARMA/ARIMA model is appropriate for the time-series. There are three forms of information criteria: the Akaike's Information Criterion (AIC), the corrected Akaike's Information Criterion (AICc), and the Bayesian Information Criterion (BIC). The model that has the least information criterion is accepted as the best model for the time-series studied It does not matter which information criterion is used as a reference when determining the most appropriate model for a given data set. However, the AICc is generally the preferred information criterion for small sample models. MATLAB's aicbic function was used to perform the calculations in this study (Box et al., 2015; Brockwell and Davis, 2016; Hyndman and Athanasopoulos, 2018).

Within the scope of the given information, a regression analysis was performed using autoregressive models in the program written in MATLAB. The GSFC Mascon time-series of the Yangtze, Murray, and Amazon basins, which are important basins for monitoring changes in water storage, were analyzed by applying different autoregressive models, and the best-fitted model was determined. Future EWT changes were forecasted based on the best-fitting model of GRACE-only data and compared with those from the GRACE-FO observations. The obtained results are discussed in the section that follows.

3. Results and discussion

Selected basins are located in different parts of the Earth. The Yangtze Basin is in the southern part of China. The Yangtze River is one of the longest rivers in the world. GSFC Mascon Basin solution contains 142 mascon cells to represent the Yangtze Basin area. The Murray–Darling Basin, located in the southeastern Australia, includes the Murray and Darling rivers. Hydrological data sets demonstrate that the Murray–Darling basin is particularly sensitive to extreme hydrological events such as floods and droughts. The Murray–Darling Basin is represented by 78 mascon cells in the GSFC Mascon Basin solutions. The Amazon Basin is located in a strategic location in South America. Groundwater storage is critical in the ecological cycles of the Amazon basin, which contains the world's largest drainage basin. It has an impact on the rainforest ecosystems as well as climate variability. Extreme climate events have occurred in the Amazon Basin that have been associated with El Nino and La Nina effects. There are 484 mascon cells for the Amazon Basin in GSFC Mascon Basin solutions. The above-mentioned basins are represented in Figure 1. When the basins are considered geographically, it is apparent that they are located in different climatic regions. Because of this, they are the focus of events that are important to different parts of the hydrological cycle, such as precipitation, droughts, or groundwater storage.

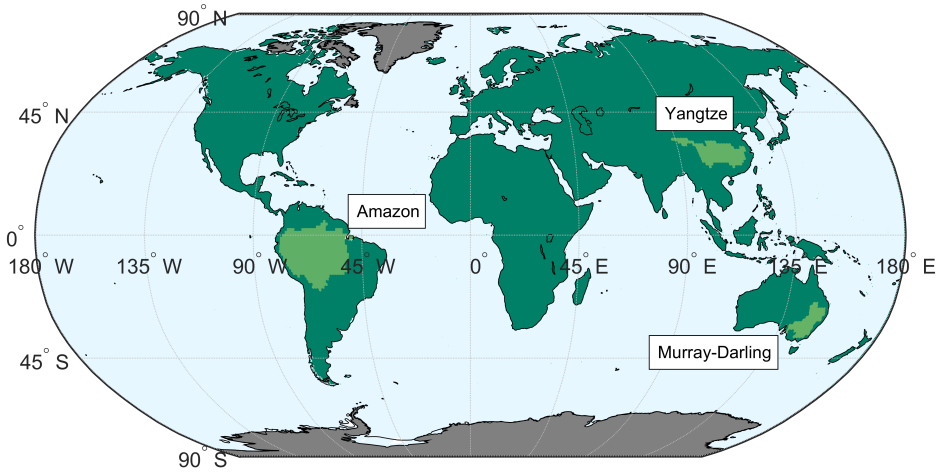

Fig. 1. Locations of the studied basins. The dark green parts correspond to lands, whereas the gray areas correspond to polar regions. The Yangtze, Murray–Darling and Amazon basins are also shown in light green

The EWT changes of three basins are given in Figure 2. Each one has different behavior in terms of EWT changes for the GRACE period. Since 2010, the Murray–Darling basin time-series has owned significant changes. This increase in EWT has been correlated to the strong precipitation events caused by La-Nina during 2010 and 2011. Floods in 2009 and 2010, which occurred as a result of hydro-climatic factors, increased the EWT in the Amazon and Yangtze basins, respectively.

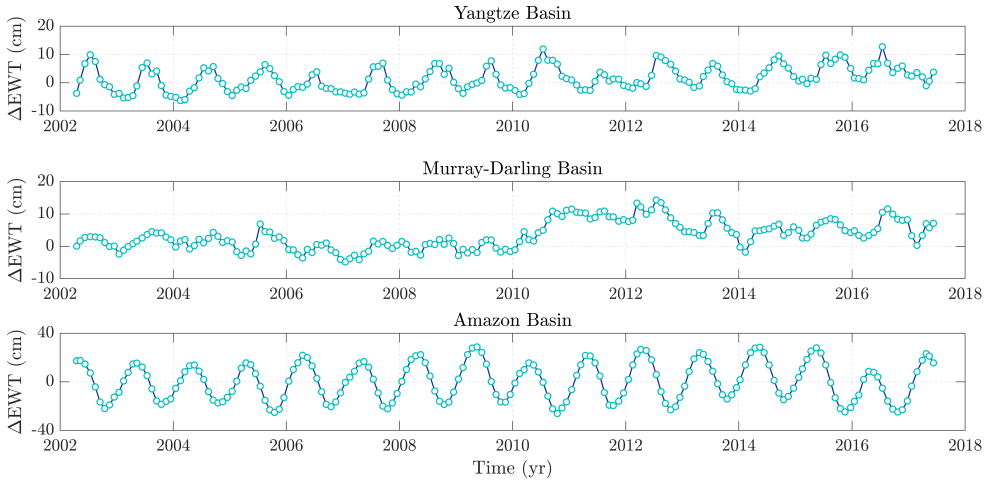

Fig. 2. GRACE EWT changes of three basins

Solutions from the GSFC Mascon Basin were only considered for the GRACE period. Firstly, analyses have been performed having assumed that the time-series includes only white noise, i.e., no temporal correlation. The harmonic regression approach given in Eq. (1) is used as a functional model to obtain the parameters with the least-square adjustment. PSD analysis was performed using the residuals obtained from the regression analysis. The negative slope of the log–log PSD graphs in Figure 3 shows the existence of colored noise, such as flicker or a random walk.

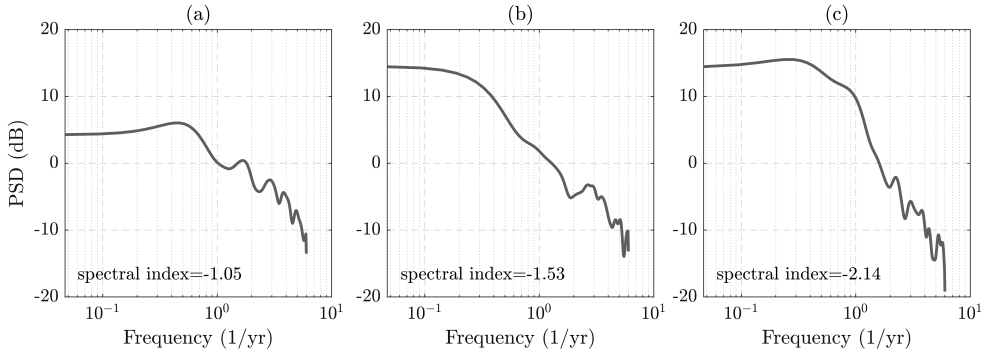

Fig. 3. Log–log graphs of the basins: (a) Yangtze, (b) Murray–Darling and (c) Amazon

Several autoregressive moving average models were used to analyze the basins after identifying that the fractional Brownian motion existed as a colored noise similar to flicker noise. We applied the ARMA(0,0), ARIMA(0,1,0), ARMA(1,0) and ARMA(1,1) models to the three basins solutions, which correspond to white noise only, random walk noise, and power-law noise. Table 1 summarizes the trend estimates and standard errors

associated with these models. Standard errors of white noise-only model (ARMA(0,0)) are generally 2–20 times lower than for the other autoregressive models, as seen in Table 1. This does not mean, however, that the ARMA(0,0) model properly explains the stochasticity of the time-series. This implies that a model considering correct noise type in the time-series provides realistic results. These more realistic results are critical in assessing the significance of the trend. According to the results of the ARMA(0,0) model, the trend values for all three basins are significant and underestimated. However, it is clear that the values are overestimated and there is no significant water mass change in the ARIMA(0,1,0). The standard errors estimated by the ARMA(1,0) and ARMA(1,1) models are approximately three times greater than that obtained by the ARMA(0,0) model. In this case, the Amazon basin trend is interpreted as insignificant.

Table 1. Statistics from autoregressive models. Unit in cm/yr

Basin	Yangtze		Murray–Darling		Amazon	
Model	Trend	Standard error	Trend	Standard error	Trend	Standard error
ARMA(0,0)	0.37	0.04	0.53	0.08	0.20	0.09
ARMA(1,0)	0.36	0.08	0.54	0.23	0.12	0.47
ARIMA(0,1,0)	0.05	1.98	0.33	1.58	0.18	1.82
ARMA(1,1)	0.36	0.07	0.53	0.22	0.14	0.37

The first step toward determining the best appropriate model is to compare the values of the information criteria listed in Table 2. The model with the minimum value is considered as the one that best fits the noise characteristics. When compared to other models in this study, the ARMA(1,1) model has the minimum information criterion. Following that, autocorrelation and partial autocorrelation plots (ACF and PCF) are also used to check the validity of the model chosen based on the information criterion, as well. These plots for Amazon basin are given in Figure 4 as an example for ARMA(1,1). As seen in Figure 4, the existing correlations at different lags of the time-series (left panel) becomes insignificant (those between blue lines) after applying ARMA(1,1) (right panel).

Table 2. Information criteria of autoregressive models for basins

	AICc values		
Model	Yangtze	Murray–Darling	Amazon
ARMA(0,0)	840.47	968.59	1137.31
ARMA(1,0)	744.39	702.58	766.61
ARIMA(0,1,0)	777.39	712.10	770.63
ARMA(1,1)	741.44	704.61	734.58

In other words, the ARMA(1,1) model provides a sufficient regression model for the parameter estimates such that the output residuals become uncorrelated. This superiority of ARMA(1,1) is valid also for the Yangtze and Murray–Darling basins. Therefore, the ARMA(1,1) model is accepted as the best model for the basins herein.

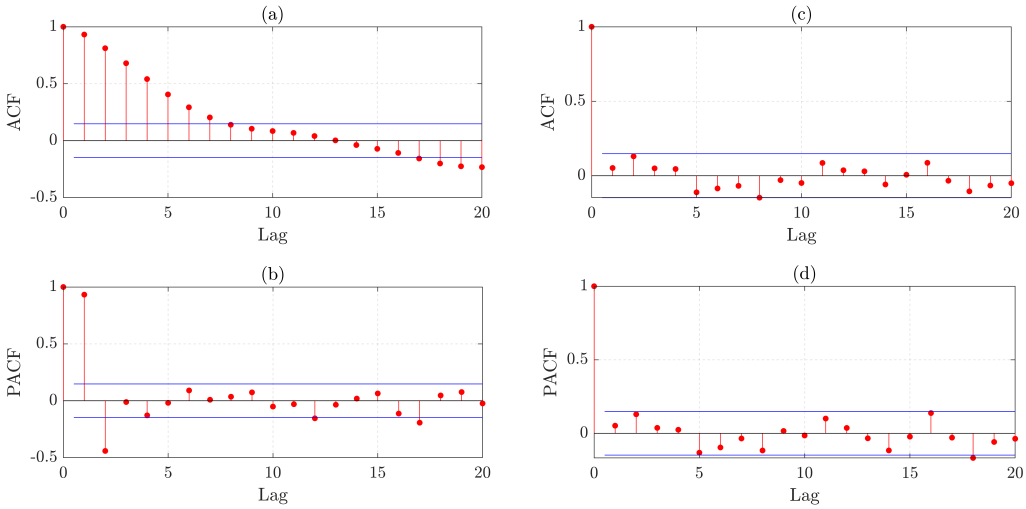

Fig. 4. ACF and PACF plots for the Amazon basin: (a) and (b) show the ARMA(0,0) model whereas (c) and (d) show ARMA(1,1) model

The harmonic regression model also yields shift and seasonal signal amplitudes, in addition to trend and standard error. Table 3 summarizes these parameters derived from ARMA(1,1), which was chosen as the best-fit model for the basins, and ARMA(0,0), which corresponds to the WN-only model solutions. When the results in Table 3 are analyzed, it can be observed that the parameters do not change quite as much as the trend and their standard error. Although the parameters defining the shift and seasonal signals do not vary, selecting the most appropriate model is important for time series analysis, as the trend significance changes. Because the model selection tells you about the whole time series and is important for predicting how the signal will move in the future, it is important to think about the model selection carefully.

Regression analysis with a proper autoregressive model gives a chance also for forecasting the changes in future within a properly defined confidence interval since the parameters and their standard errors in the regression model are unbiasedly estimated. In order to check how our ARMA(1,1) model for the basins works well, the future EWT changes (between 2017 and mid of 2021) are forecasted with their 95% confidence intervals and compared with those from GRACE-FO data which starts from the mid of 2018. Correlation coefficients between GRACE-FO observations and ARMA(1,1) model predictions were calculated. Using MATLAB's corrcoef tool, Pearson correlation coefficient (PCC) were determined to be 0.61, 0.97, and 0.33 for the Yangtze, Murray–Darling and Amazon basins, respectively. The forecast results associated with the Yangtze and Amazon basins shown in Figure 5a and Figure 5c are compatible with those from

Table 3. Parameters from autoregressive models

Yangtze basin					
Model	Shift	Annual amplitude		Semi-annual amplitude	
		cosine	sine	cosine	sine
ARMA(0,0)	−1.32 ± 0.38	4.37 (cm)		0.88 (cm)	
		−1.98 ± 0.26	3.89 ± 0.29	−0.84 ± 0.27	−0.25 ± 0.27
ARMA(1,1)	−1.32 ± 0.67	4.34 (cm)		0.86 (cm)	
		−1.98 ± 0.42	3.86 ± 0.44	−0.83 ± 0.30	−0.23 ± 0.26
Murray–Darling basin					
Model	Shift	Annual amplitude		Semi-annual amplitude	
		cosine	sine	cosine	sine
ARMA(0,0)	−0.56 ± 0.71	2.09 (cm)		0.46 (cm)	
		−1.28 ± 0.37	1.66 ± 0.35	−0.29 ± 0.34	−0.35 ± 0.36
ARMA(1,1)	−0.67 ± 2.16	2.08 (cm)		0.44 (cm)	
		−1.29 ± 0.36	1.63 ± 0.41	−0.33 ± 0.19	−0.29 ± 0.20
Amazon basin					
Model	Shift	Annual amplitude		Semi-annual amplitude	
		cosine	sine	cosine	sine
ARMA(0,0)	−1.38 ± 1.09	20.32 (cm)		0.99 (cm)	
		20.02 ± 0.60	3.45 ± 0.56	−0.38 ± 0.57	0.92 ± 0.55
ARMA(1,1)	−0.96 ± 3.40	20.31 (cm)		1.06 (cm)	
		20.00 ± 0.56	3.53 ± 0.54	−0.40 ± 0.25	0.98 ± 0.25

GRACE-FO. Most importantly, the estimated confidence interval from the ARMA(1,1) model for the Yangtze basin also covers the irregular variations of the EWT changes in the GRACE-FO data. This implies how the ARMA(1,1) model provides proper parameter estimates with realistic standard errors. On the other hand, the forecast does not work for Murray–Darling basin as efficient as the other basins even though the lower part of the confidence region shows the similar behavior of the GRACE-FO ones as seen in Figure 5b.

It is worth noting that this mismatch is due to the missing functional model for the Murray–Darling basin which is under the abnormal climatic effects such as La-Nina and El-Nino events. Therefore, we applied three ARIMA models to this basin. The obtained trend results and the AICc values from these models are given in Table 4. The best result is obtained with the ARIMA(1,1,1). However, the trend estimates (nearly 0.33 cm/yr) are all insignificant. On the other hand, the prediction confidence interval of the ARIMA(1,1,1) coincides with the GRACE-FO signal. This shows that the ARIMA(1,1,1) yields more

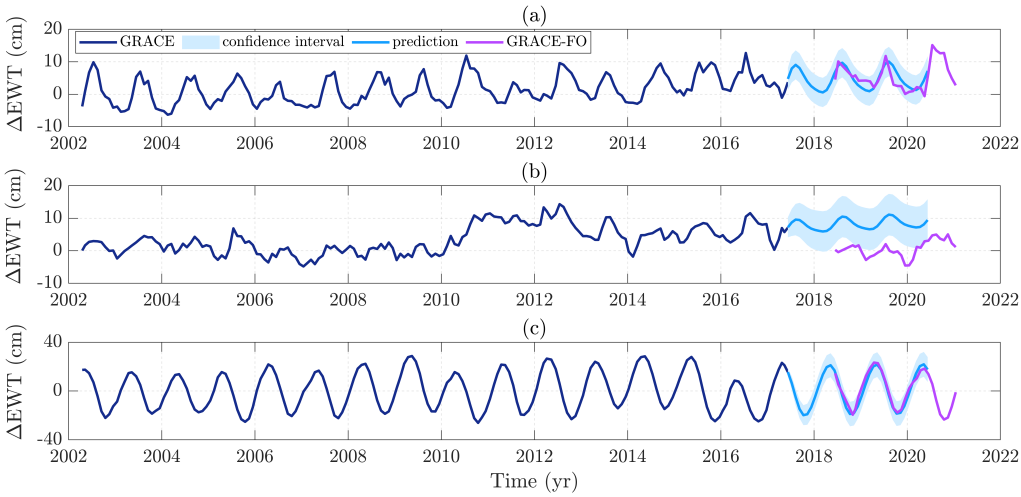

Fig. 5. Forecasts with 95% confidence level derived from the ARMA(1,1) model for the basins: (a) Yangtze, (b) Murray–Darling, and (c) Amazon

reliable result for this basin than the ARMA(1,1), see Figure 6. However, it is worth mentioning that this basin needs further investigation due to the different hydrological signals existing in the GRACE/GRACE-FO time-series.

Table 4. Statistics from autoregressive models for Murray–Darling basin

Model	Trend (cm/yr)	Standard error (cm/yr)	AICc
ARIMA(1,1,0)	0.32	1.53	714.02
ARIMA(0,1,1)	0.32	1.45	713.63
ARIMA(1,1,1)	0.33	0.77	707.63

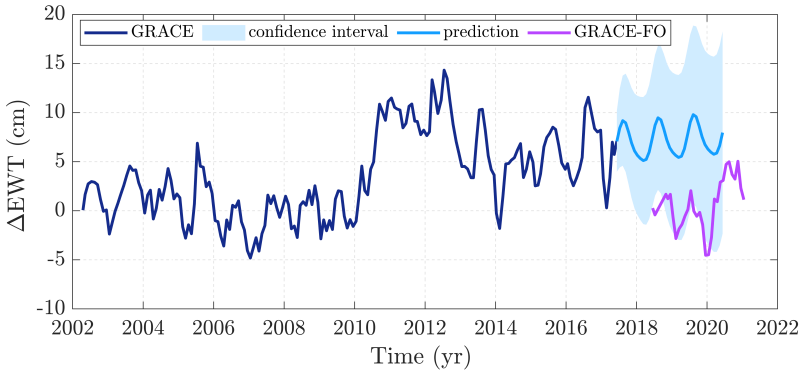

Fig. 6. Forecasts with 95% confidence level derived from the ARIMA(1,1,1) model for the Murray–Darling basin

4. Conclusions

This study examines how to model the noise in a GRACE-Mascon derived EWT time-series using autoregressive models. For this aim, the Yangtze, Murray–Darling, and Amazon basins are considered. First, it is shown that the GRACE time-series contains temporal correlations causing colored noise in the data. According to the numerical results on the basins, it has been obtained that the ARMA(1,1) model is the best-fitting noise model. This model corresponds to power-low noise, which is a part of Brownian motion, similar to flicker noise. The ARMA(1,1) model yields about four times bigger standard errors than the ARMA(0,0) model which actually corresponds to the standard regression analysis without weighting applied mostly in practice. It means that the standard analysis causes underestimate in the uncertainty of the parameters from GRACE EWT-time series. The convenience of the estimates from ARMA(1,1) model is tested by comparing the forecasted EWT changes with those from GRACE-FO data which is not involved in the autoregression. The results for the Yangtze and Amazon basins are very promising for modeling the noise in GRACE time-series whereas the Murray–Darling basin needs further modelling including the floods and droughts in the region. Accordingly, the ARMA models improve the reliability of the estimates in the GRACE time-series. Our autoregression model will be improved in future studies such that it also consists of basin-related physical components in addition to the others in the standard regression model for GRACE time-series.

Author contributions

Conceptualization: O.G. and C.A.; methodology development: O.G. and C.A.; writing – original draft: O.G. and C.A.; writing – review and editing: O.G. and C.A.

Data availability statement

GRACE mascon data sets are available at the Goddard Earth Science Research GRACE Mascon Current Products webpages (https://earth.gsfc.nasa.gov/geo/data/grace-mascons).

Acknowledgements

The authors thank NASA/GSFC for providing GRACE Mascon solutions. Analysis and maps in this study were created using MATLAB R2021b, licensed on behalf of Yildiz Technical University. This work was supported by Yildiz Technical University Scientific Research Projects Coordination Unit under project number FDK-2021-4341.

References

Ahmed, M., Sultan, M., Elbayoumi, T. et al. (2019). Forecasting grace data over the African watersheds using artificial neural networks. *Remote Sens.*, 11(15), 1769. DOI: 10.3390/rs11151769.

Baur, O. (2012). On the computation of mass-change trends from GRACE gravity field time-series. *J. Geodyn.*, 61, 120–128. DOI: 10.1016/j.jog.2012.03.007.

Becker, M., Meyssignac, B., Xavier, L. et al. (2011). Past terrestrial water storage (1980–2008) in the Amazon Basin reconstructed from GRACE and in situ river gauging data. *Hydrol. Earth Syst. Sci.*, 15(2), 533–546. DOI: 10.5194/hess-15-533-2011.

Birylo, M., Rzepecka, Z., Kuczynska-Siehien, J. et al. (2018). Analysis of water budget prediction accuracy using ARIMA models. *Water Sci. Technol. Water Supply*, 18(3), 819–830. DOI: 10.2166/ws.2017.156.

Boergens, E., Kvas, A., Eicker, A. et al. (2022). Uncertainties of GRACE-Based Terrestrial Water Storage Anomalies for Arbitrary Averaging Regions. *J. Geophys. Res. Solid Earth*, e2021JB022081. DOI: 10.1029/2021JB022081.

Box, G.E.P., Jenkins, G.M., Reinsel, G.C. et al. (2015). *Time-series analysis: Forecasting and control. (5th ed.)*. New Jersey: John Wiley & Sons.

Brockwell, P.J., and Davis, R.A. (2016). *Introduction to time-series and forecasting (3rd ed.)*. New York: Springer.

Brown, N.J., and Tregoning, P. (2010). Quantifying GRACE data contamination effects on hydrological analysis in the Murray–Darling Basin, southeast Australia. *Aust. J. Earth Sci.*, 57(3), 329–335. DOI: 10.1080/08120091003619241.

Cazenave, A., and Chen, J. (2010). Time-variable gravity from space and present-day mass redistribution in the earth system. *Earth Planet. Sci. Lett.*, 298, 263–274. DOI: 10.1016/j.epsl.2010.07.035.

Chao, N., and Wang, Z. (2017). Characterized flood potential in the Yangtze River basin from GRACE gravity observation, hydrological model and in-situ hydrological station. *J. Hydrol. Eng.*, 22(9), 05017016. DOI: 10.1061/(ASCE)HE.1943-5584.0001547.

Chao, N., Jin, T., Cai, Z. et al. (2021). Estimation of component contributions to total terrestrial water storage change in the Yangtze River basin. *J. Hydrol.*, 595, 125661. DOI: 10.1016/j.jhydrol.2020.125661.

Chatfield, C. (2003). *The analysis of time series: An introduction (6th ed.)*. London: Chapman and Hall CRC.

Chen, J.L., Wilson, C.R., and Tapley, B.D. (2010). The 2009 exceptional Amazon flood and interannual terrestrial water storage change observed by GRACE. *Water Resour. Res.*, 46(12). DOI: 10.1029/2010WR009383.

Chen, J., Tapley, B., Rodell, M. et al. (2020). Basin scale river runoff estimation from GRACE gravity satellites, climate models, and in situ observations: A case study in the Amazon basin. *Water Resour. Res.*, 56(10), e2020WR028032. DOI: 10.1029/2020WR028032.

Chen, J., Cazenave, A., Dahle, C. et al. (2022). Applications and Challenges of GRACE and GRACE Follow-On Satellite Gravimetry. *Surv. Geophys.*, 1–41. DOI: 10.1007/s10712-021-09685-x.

Crowley, J.W., Mitrovica, J.X., Bailey, R.C. et al. (2008). Annual variations in water storage and precipitation in the Amazon Basin. *J. Geod.*, 82(1), 9–13. DOI: 10.1007/s00190-007-0153-1.

Davis, J.L., Wernicke, B.P., and Tamisiea, M.E. (2012). On seasonal signals in geodetic time series. *J. Geophys. Res. Solid Earth*, 117(B1). DOI: 10.1029/2011JB008690.

Dobslaw, H., Bergmann-Wolf, I., Dill, R. et al. (2017). Product Description Document for AOD1B Release 06, GRACE 327-750, GFZ German Research Centre for Geosciences, Department 1: Geodesy and Remote Sensing. Retrieved from https://podaac-tools.jpl.nasa.gov/drive/files/allData/gracefo/docs/AOD1B_PDD_RL06_v6.1.pdf.

Famiglietti, J.S., and Rodell, M. (2013). Water in the balance. *Science*, 340(6138), 1300–1301. DOI: 10.1126/science.1236460.

Fasullo, J.T., Boening, C., Landerer, F.W. et al. (2013). Australia's unique influence on global sea level in 2010-2011. *Geophys. Res. Lett.*, 40(16), 4368–4373. DOI: 10.1002/grl.50834.

Ferreira, V.G., Gong, Z., He, X. et al. (2013). Estimating total discharge in the Yangtze River Basin using satellite-based observations. *Remote Sens.*, 5(7), 3415–3430. DOI: 10.3390/rs5073415.

Forsberg. R., Sørensen, L., and Simonsen, S. (2017). Greenland and Antarctica ice sheet mass changes and effects on global sea level. *Surv. Geophys.*, 38(1), 89–104. DOI: 10.1007/s10712-016-9398-7.

Frappart, F., Papa, F., da Silva, J.S. et al. (2012). Surface freshwater storage and dynamics in the Amazon basin during the 2005 exceptional drought. *Environ. Res. Lett.*, 7(4), 044010. DOI: 10.1088/1748-9326/7/4/044010.

Frappart, F., and Ramillien, G. (2018). Monitoring groundwater storage changes using the Gravity Recovery and Climate Experiment (GRACE) satellite mission: A review. *Remote Sens.*, 10(6), 829. DOI: 10.3390/rs10060829.

Frappart, F., Papa, F., Güntner, A. et al. (2019). The spatio-temporal variability of groundwater storage in the Amazon River Basin. *Adv. Water Resour.*, 124, 41–52. DOI: 10.1016/j.advwatres.2018.12.005.

Gao, Z., Long, D., Tang, G. et al. (2017). Assessing the potential of satellite-based precipitation estimates for flood frequency analysis in ungauged or poorly gauged tributaries of China's Yangtze River basin. *J. Hydrol.*, 550, 478–496. DOI: 10.1016/j.jhydrol.2017.05.025.

Guo, X., Zhao, Q., Ditmar, P. et al. (2018). Improvements in the monthly gravity field solutions through modeling the colored noise in the GRACE data. *J. Geophys. Res. Solid Earth*, 123(8). DOI: 10.1029/2018JB015601.

Heimhuber, V., Tulbure, M.G., Broich, M. et al. (2019). The role of GRACE total water storage anomalies, streamflow and rainfall in stream salinity trends across Australia's Murray–Darling Basin during and post the Millennium Drought. *Int. J. Appl. Earth Obs. Geoinf.*, 83, 101927. DOI: 10.1016/j.jag.2019.101927.

Huang, Y., Salama, M.S., Krol, M.S. et al. (2015). Estimation of human induced changes in terrestrial water storage through integration of GRACE satellite detection and hydrological modeling: a case study of the Yangtze River basin. *Water Resour Res*. 51, 8494–8516. DOI: 10.1002/2015WR016923.

Huang, P., Song, J., Cheng, D. et al. (2021). Understanding the intra-annual variability of streamflow by incorporating terrestrial water storage from GRACE into the Budyko framework in the Qinba Mountains. *J. Hydrol.*, 603, 126988. DOI: 10.1016/j.jhydrol.2021.126988.

Hyndman, R.J., and Athanasopoulos, G. (2018). *Forecasting: principles and practice (2nd ed.)*. OTexts.

King, M.A., and Watson, C.S. (2020). Antarctic surface mass balance: Natural variability, noise, and detecting new trends. *Geophys. Res. Lett.*, 47(12), e2020GL087493. DOI: 10.1029/2020GL08749.

Loomis, B.D., Luthcke, S.B., and Sabaka T.J. (2019). Regularization and error characterization of GRACE mascons. *J. Geod.*, 93(9), 1381–1398. DOI: 10.1007/s00190-019-01252-y.

Loomis, B.D., Rachlin, K.E., Wiese, D.N. et al. (2020). Replacing GRACE/GRACE-FO with satellite laser ranging: Impacts on Antarctic Ice Sheet mass change. *Geophys. Res. Lett.*, 47(3). DOI: e2019GL085488.

Luthcke, S.B., Sabaka, T.J., Loomis, B.D. et al. (2013). Antarctica, Greenland and Gulf of Alaska land-ice evolution from an iterated GRACE global mascon solution. *J. Glaciol.*, 59(216), 613–631. DOI: 10.3189/2013JoG12J147.

Mandelbrot, B., and Van Ness, J. (1968). Fractional brownian motions, fractional noises and applications. *SIAM Rev.*, 10, 422–437.

Pellet, V., Aires, F., and Yamazaki, D. (2021). Coherent satellite monitoring of the water cycle over the Amazon. Part 2: Total water storage change and river discharge estimation. *Water Resour. Res.*, 57, e2020WR028648. DOI: 10.1029/2020WR028648.

Peltier, W.R., Argus, D.F., and Drummond, R. (2015). Space geodesy constrains ice-age terminal deglaciation: The global ICE-6G C (VM5a) model. *J. Geophys. Res. Solid Earth*, 120, 450–487. DOI: 10.1002/2014JB011176.

Rahaman, M.M., Thakur, B., Kalra, A. et al. (2019). Modeling of GRACE-derived groundwater information in the Colorado River Basin. *Hydrology*, 6(1), 19. DOI: 10.3390/hydrology6010019.

Ran, J., Ditmar, P., Klees R. et al. (2018). Statistically optimal estimation of Greenland ice sheet mass variations from GRACE monthly solutions using an improved mascon approach. *J. Geod.*, 92(3), 299–319. DOI: 10.1007/s00190-017-1063-5.

Ries, J., Bettadpur, S., Eanes, R. et al. (2016). The Combined Gravity Model GGM05C. GFZ Data Services. DOI: 10.5880/icgem.2016.002.

Scanlon, B.R., Rateb, A., Anyamba, A. et al. (2022). Linkages between GRACE water storage, hydrologic extremes, and climate teleconnections in major African aquifers. *Environ. Res. Lett.*, 17(1), 014046. DOI: 10.18738/T8/HLXCMY.

Schumacher, M., Forootan, E., van Dijk, A.I. et al. (2018). Improving drought simulations within the Murray–Darling Basin by combined calibration/assimilation of GRACE data into the WaterGAP Global Hydrology Model. *Remote Sens. Environ.*, 204, 212–228. DOI: 10.1016/j.rse.2017.10.029.

Sun, Z., Zhu, X., Pan, Y. et al. (2017). Assessing terrestrial water storage and flood potential using GRACE data in the Yangtze River basin, China. *Remote Sens.*, 9(10), 1011. DOI: 10.3390/rs9101011.

Tapley, B.D., Bettadpur, S., Watkins, M. et al. (2004). The gravity recovery and climate experiment: Mission overview and early results. *Geophys. Res. Lett.*, 31(9). DOI: 10.1029/2004GL019920.

Tapley, B.D., Watkins, M.M., Flechtner, F. et al. (2019). Contributions of GRACE to understanding climate change. *Nat. Clim. Change.*, 9(5), 358–369. DOI: 10.1038/s41558-019-0456-2.

Wahr, J., Swenson, S., and Velicogna, I. (2006). Accuracy of GRACE mass estimates. *Geophys. Res. Lett.*, 33(6). DOI: 10.1029/2005GL025305.

Wang, L., Chen, C., Ma, X. et al. (2020). Evaluation of GRACE mascon solutions using in-situ geodetic data: The case of hydrologic-induced crust displacement in the Yangtze River Basin. *Sci. Total Environ.*, 707, 135606. DOI: 10.1016/j.scitotenv.2019.135829.

Welch, P.D. (1967). The use of fast fourier transform for the estimation of power spectra: a method based on time averaging over short, modified periodograms. *IEEE trans. audio electroacoust*. 15(2), 70–73. DOI: 10.1109/TAU.1967.1161901.

Williams, S.D.P., Moore, P., King, M.A. et al. (2014). Revisiting GRACE Antarctic ice mass trends and accelerations considering autocorrelation. *Earth Planet. Sci. Lett.*, 385, 12–21. DOI: 10.1016/j.epsl.2013.10.016.

Xie, Z., Huete, A., Restrepo-Coupe, N. et al. (2016). Spatial partitioning and temporal evolution of Australia's total water storage under extreme hydroclimatic impacts. *Remote Sens. Environ.*, 183, 43–52. DOI: 10.1016/j.rse.2016.05.017.

Yin, H., and Li, C. (2001). Human impact on floods and flood disasters on the Yangtze River. *Geomorphology*, 41(2-3), 105–109. DOI: 10.1016/S0169-555X(01)00108-8.

Zhang, Y., He, B.I.N., Guo, L. et al. (2019). Differences in response of terrestrial water storage components to precipitation over 168 global river basins. *J. Hydrometeorol.*, 20(9), 1981–1999. DOI: 10.1175/JHM-D-18-0253.1.

Zhou, Y., Jin, S., Tenzer, R. et al. (2016). Water storage variations in the Poyang Lake Basin estimated from GRACE and satellite altimetry. *Geod. Geodyn.*, 7(2), 108–116. DOI: 10.1016/j.geog.2016.04.003.